Some Phase-Diagram Aspects of the Manganese-Carbon System

DU SICHEN, S. SEETHARAMAN, and L.-I. STAFFANSSON

In the present work, differential thermal analysis (DTA) and electromotive force (emf) methods were employed to investigate the Mn-C phase diagram around the eutectoid decomposition of Mn(γ). The eutectoid temperature and the composition were estimated to be 1031 K and 9.62 mol pct carbon, respectively. The temperature for the eutectoid decomposition of ε-carbide to Mn(γ) and $Mn_{23}C_6$ was found to be 1260 K, and the equilibrium composition of Mn(γ) corresponding to this three-phase reaction was 14.89 mol pct carbon. From the experimental data, the solubility of $Mn_{23}C_6$ in Mn(γ) was evaluated in the temperature range of 1031 to 1260 K using a two-sublattice model. On the basis of the present results, the relevant part of the Mn-C diagram was redrawn. Microscopic and X-ray analyses of quenched samples appear to be in support of the suggested phase diagram.

I. INTRODUCTION

A knowledge of the phase equilibria in the manganese-carbon system is of great importance in understanding the properties of alloy steels. The earliest systematic investigation of the system has been carried out by Vogel and Döring.[1] This was followed up by the even more detailed studies of Isobe[2] and Kuo and Persson.[3] The results of latter studies differ significantly from those of Vogel and Döring. Benz *et al.*[4] have carried out extensive X-ray diffraction and microscopic studies of the Mn-C binary system in the temperature range of 973 to 1173 K. The present version of the phase diagram,[5] represented in Figure 1, is based on the results of Kuo and Persson,[3] Benz *et al.*,[4] and Bouchaud.[6]

There are a number of uncertainties concerning the phase diagram in Figure 1, especially in the solid-state region with carbon content less than 5.39 wt pct. For example, the decomposition temperature of Mn(γ) solid solution has been variously reported as 1013,[1] 1093,[2] and 1163 K.[4] Such discrepancies could be attributed to traces of impurities in the starting materials and to experimental difficulties. Actually, the Mn-C alloys are hygroscopic in nature, and they are susceptible to oxidation as well. Further, a number of earlier investigators[2-4,6,7] have reported serious experimental difficulties in retaining the high-temperature phases by quenching methods, as the phase transformations involved are extremely fast. The present work was aimed at a detailed study of the eutectoid reaction

$$Mn(\gamma) = Mn(\alpha) + Mn_{23}C_6 \qquad [1]$$

in order to determine the temperature of the three-phase reaction, the eutectoid composition as well as the solubility of $Mn_{23}C_6$ in Mn(γ). The experimental techniques involved were DTA, solid-state galvanic cell measurements with CaF_2 as electrolyte, microscopic examination, and X-ray analysis. A two-sublattice regular solution model[8] was used in the theoretical analysis of the experimental results.

DU SICHEN, Graduate Student, S. SEETHARAMAN, Docent and Senior Lecturer, and L.-I. STAFFANSSON, Professor, are with the Department of Theoretical Metallurgy, The Royal Institute of Technology, S-100 44 Stockholm, Sweden.

Manuscript submitted October 21, 1988.

II. EXPERIMENTAL

A. *Materials*

Pure Mn powder (99.9 pct, E. Merck, Darmstadt, Federal Republic of Germany), having a particle size of less than 150 μm, and specpure graphite powder of pelletable quality (Johnson Matthey Ltd., Royston, United Kingdom) were used in the preparation of the Mn-C alloys. Single crystals of CaF_2 (15 mm in diameter and 5 mm in thickness) (Harshaw Chemie Bv, Be Meern, The Netherlands) were used as electrolytes. CaF_2 powder (suprapure, E. Merck Federal Republic of Germany) and MnF_2 powder (Ventron Alpha Produkte, Karlsruhe, Federal Republic of Germany) were used in the preparation of electrodes in the galvanic cell. Both CaF_2 and MnF_2 powders were dried at 673 K in vacuum (2×10^{-5} bar) for 12 hours before use. Aluminum oxide powder (standardized for chromatographic adsorption analysis, E. Merck) was used as reference material for DTA analysis. This was calcined before being used in the experiments. The argon gas (SR grade), as well as argon-1 pct hydrogen gas mixture used in the present work, was supplied by AGA Special Gas, Stockholm, Sweden. Both gases were purified by using the procedure described earlier.[9] The oxygen partial pressures in the gases were constantly monitored by ZrO_2-CaO solid electrolyte galvanic cells during the experiments. The values of p_{O_2} in the gases after purification were found to be less than 10^{-22} bar.

B. *Preparation of the Mn-C Alloys*

Manganese and graphite powders were mixed thoroughly in required proportions in an agate mortar to get the desired compositions. For DTA and emf studies, the samples were prepared by pressing the mixtures into pellets and sintering them in a closed boron nitride crucible in a stream of purified argon at 1323 K for 48 hours. These sintering conditions have been shown by Kuo and Persson[3] to be adequate for the completion of the

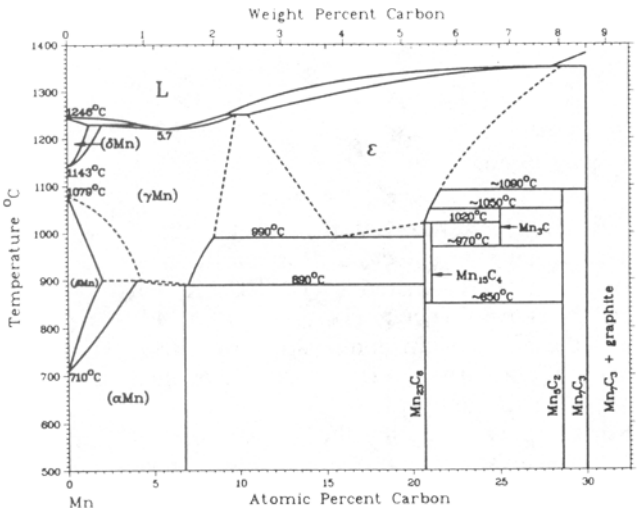

Fig. 1—Mn-C phase diagram.

reaction. To obtain dense samples for heat treatment, some mixtures were melted in ZrO_2 crucibles in a purified argon stream. Both sintered and melted samples were cooled in the furnace itself. The carbon content obtained by analysis was in agreement with the weighed in amounts within ±2 pct.

C. *Differential Thermal Analysis*

The DTA measurements were performed using a Mettler thermoanalyzer. A Pt-10 pct Rh/Pt thermocouple arrangement was used for these studies. The Mn-C alloy was first crushed and finely ground in a glove box under argon atmosphere. About 0.8 g of the sample was then compacted into an alumina crucible with a lid. A similar crucible containing about 0.8 g of alumina powder was used as the reference.

After mounting the sample and the reference on the crucible holder with the thermocouple arrangement, as shown in Figure 2, the apparatus was evacuated and filled with purified Ar-1 pct H_2 gas mixture. The system was then flushed with the gas mixture for at least 3 hours. The gas flow was then decreased to about 100 ml/min and was kept constant during the entire measurement. When the oxygen sensor connected to the outgoing gas showed a value of p_{O_2} less than 10^{-22} bar, the heating program was started. The oxygen level in the vicinity of the sample was lowered further at high temperatures by keeping Zr-Ti alloy getters *in situ*. The weight changes of the sample were followed by means of the thermogravimetric part of the thermoanalyzer (accuracy: ±0.0001 g), and it was found that the weight changes were negligible during the course of the experiment, thereby indicating that the oxidation of C or Mn or the loss of Mn due to vaporization are negligible.

During the DTA run, the temperature was first raised to 923 K at a rate of 10 K/min and then maintained at this temperature for 1 hour. The sample was then taken through temperature cycles between 923 and 1373 K several times, and the DTA pattern was registered continuously. The heating and cooling rates were generally kept at 6 K/min. Even though this rate was found to be convenient, changing of the heating and cooling rates to

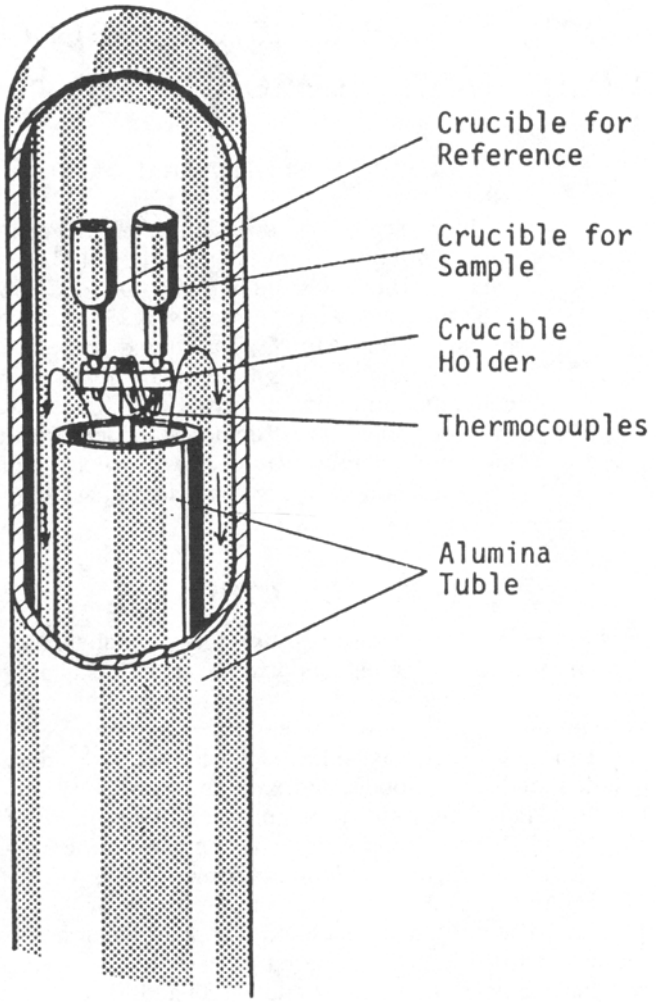

Fig. 2—The DTA arrangement.

10 K/min or 4 K/min in the case of some of the experiments did not affect the experimental results. The thermocouple arrangement was calibrated before and after each experiment against the melting points of pure aluminum and gold under identical conditions, and the experimental temperatures were corrected using the calibration curves. It was found that the calibration curves remained unaltered during the course of the entire experimental series.

D. *Emf Measurements*

The galvanic cell arrangement and the experimental procedure for emf measurements have been described in detail in a previous work.[9] The galvanic cell used in the present work can be represented as

$$(-)\ \text{Mn},\ \text{MnF}_2,\ \text{CaF}_2 \parallel \text{CaF}_2 \parallel \text{CaF}_2,\ \text{MnF}_2,\ \text{“Mn-C”}\ (+) \qquad [\text{I}]$$

the cell reaction being

$$\text{Mn} \rightarrow \underline{\text{Mn}}\ (\text{Mn-C alloy}) \qquad [2]$$

The CaF_2 electrolyte pellet was kept sandwiched between the two electrodes in an open cell arrangement.

The cell was placed in a vertically mounted alumina reaction tube and was positioned in the even temperature zone of the furnace (±1 K over a length of 5 cm). An oxygen partial pressure of less than 10^{-22} bar was maintained in the reaction tube by passing a stream of purified argon gas constantly through the reaction tube. The cell emf was measured to an accuracy of ±0.01 mV by a Newport millivoltmeter with an input impedance of 10^9 ohms and was registered by a Newport digital printer. The emf values were considered to be steady if they were constant within ±0.1 mV over a period of 3 hours.

E. *Microscopic and X-Ray Studies*

The samples for microscopic and X-ray studies were prepared as follows. The dense alloy samples were embedded in Al_2O_3 powder kept in quartz crucibles and were sealed under vacuum. The alumina powder prevented any possible reaction between quartz and the samples. The specimens were heated up and kept at the desired temperatures for 120 hours. The samples were then quenched by dropping the capsules into salt water and crushing them immediately. X-ray analysis of the samples was carried out in a Guinier-Hägg camera using Cr as the target.

III. RESULTS

A. *DTA Measurements*

Ten different Mn-C alloys were studied by the DTA method. The temperatures corresponding to the peaks in the DTA curves for various alloys are listed in Table I. These temperatures were reproducible for various runs with the same alloy both during heating and cooling. In general, two different peaks were observed. In the case of alloy 1, a third peak was observed corresponding to 1286 K.

The first DTA peak for all the compositions was observed between 1027 and 1034 K. The average temperature for this transformation was estimated to be 1031 ± 4 K in the composition range X_C = 0.0858 to 0.1889.

For alloys 1 through 3, the second peak was observed at 1260 ± 1 K, and this peak was independent of composition in the composition range X_C = 0.1609 to 0.1889. On the other hand, for the alloys 4 through 8, the temperature of the second peak was found to vary with the composition, decreasing as the carbon content decreased, as can be seen in Table I. In the case of alloys 9 and 10, the second peak started showing an increase with decreasing carbon content.

Table I. The Results of the Differential Thermal Analysis Measurements

	Alloy Composition		Temperatures of the DTA Peaks, K		
Alloy	Wt Pct C	X_C	First Peak	Second Peak	Third Peak
1	4.84	0.1889	1031	1261	1286
2	4.59	0.1805	1032	1261	—
3	4.02	0.1609	1028	1259	—
4	3.50	0.1424	1034	1234	—
5	3.48	0.1417	1027	1227	—
6	2.90	0.1203	1032	1129	—
7	2.81	0.1169	1029	1126	—
8	2.64	0.1106	1030	1091	—
9	2.21	0.0938	1032	1093	—
10	2.01	0.0858	1032	1111	—

The results of DTA measurements have been plotted in Figure 3. It is seen that there is a clear indication of an eutectoid reaction, the temperature for the three-phase reaction being 1031 K. The eutectoid composition appears to be around X_C = 0.10. This representation in Figure 3 appears to be different from the Mn-C phase diagram given in Figure 1. In view of the uncertainties in the phase-diagram studies carried out earlier regarding the decomposition temperature of Mn(γ), as pointed out in the Introduction, it was felt that it was reasonable to mark the eutectoid reaction corresponding to reaction [1] in a tentative manner. The various single- or two-phase regions have been marked correspondingly in Figure 3. It is admitted at this stage that verification of this by other experimental methods was necessary before it could be accepted as conclusive.

In the case of alloys 1 through 3, the second peak at 1260 K appears to correspond to the decomposition temperature of ε-carbide, which has been represented as 1263 K in Figure 1.

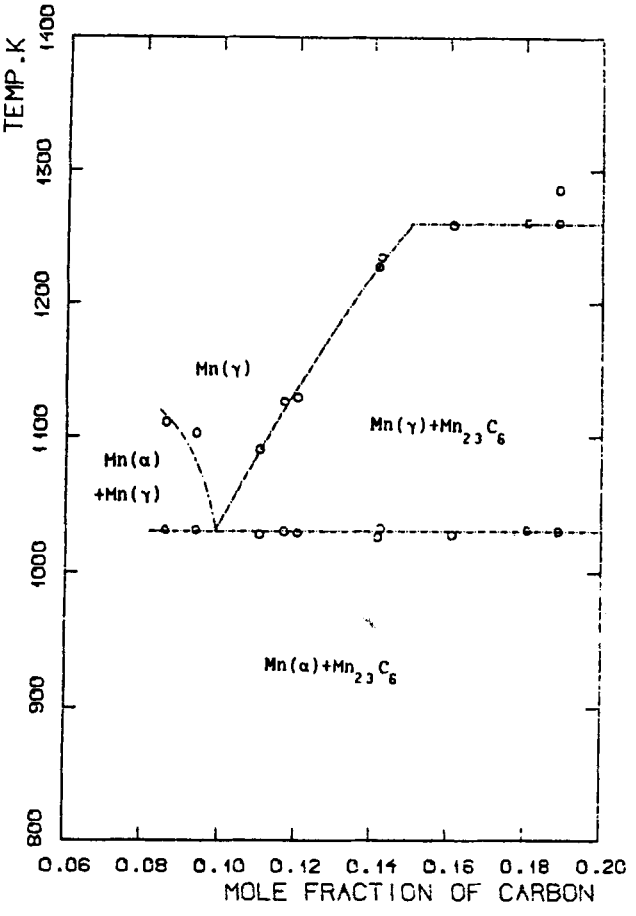

Fig. 3—The tentative phase diagram from DTA measurements.

B. *Emf Measurements*

Three different Mn-C alloys were studied in the present work by the solid-state galvanic cell method involving CaF_2 electrolyte. The alloy compositions as well as emf values obtained at various temperatures for these alloys have been listed in Table II. All three alloys were planned to be in the Mn(α)-$Mn_{23}C_6$ two-phase field at "low temperatures" according to the phase diagram in Figure 1. The galvanic cell could be represented as

$$(-)\ \text{Mn}(\alpha \text{ or } \beta),\ MnF_2,\ CaF_2 \parallel CaF_2 \parallel$$
$$CaF_2,\ MnF_2,\ \text{Mn}(\alpha)\text{-}Mn_{23}C_6\ (+) \qquad [II]$$

the cell reaction being

$$\text{Mn}(\alpha \text{ or } \beta) = \underline{\text{Mn}}\ (\text{Mn}(\alpha)\text{-}Mn_{23}C_6) \qquad [3]$$

below the eutectoid temperature.

Table II. The Results of the Galvanic Cell Measurements

Cell	Alloy Composition Wt Pct C	Alloy Composition X_C	Temperature, K	Emf, mV
I	3.50	0.1424	907	4.10
			935	4.30
			958	4.40
			978	4.30
			991.5	4.40
			1021	4.30
			1028	4.20
			1037	4.80
			1079	4.80
			1114.5	6.30
			1144	7.00
			1158	7.30
			1187	8.70
			1198.5	8.80
			1223	9.00
II	4.22	0.1679	925	4.00
			963	3.90
			985	3.90
			1007	3.80
			1042	3.90
			1084	5.30
			1107	6.10
			1157	6.40
			1174	6.90
			1195.5	7.80
			1221	8.80
III	2.01	0.0858	914	3.70
			940.5	3.70
			960	4.20
			1002	4.10
			1017	3.70
			1039	3.70
			1079	3.50
			1098	3.40
			1104	3.50
			1128.5	3.80
			1143.5	3.80
			1189	4.90
			1200	4.70
			1225	5.40
			1241	5.50

For the alloys with $X_C = 0.1424$ and $X_C = 0.1679$, the cell emf values have been plotted as a function of temperature in Figure 4. It is seen that both cells show a distinct break in the emf/temperature relationship at 1038 K, thereby indicating the occurrence of a phase transformation at this temperature. The agreement between the results for both alloys indicates that they both lie in the same phase regions in the phase diagram above as well as below the transformation temperature. Comparison with the results of the DTA measurements in Figure 3 suggests that this phase transformation could correspond to the three-phase reaction [1]. This would mean that below the transformation temperature, the alloy electrodes would consist of Mn(α) and $Mn_{23}C_6$, while above this temperature, Mn(γ) and $Mn_{23}C_6$. The difference in the eutectoid temperature obtained from the different techniques could be attributed to the experimental uncertainties.

The equation for the straight line below 1038 K can be represented as

$$E\ (\text{mV}) = 3.90(\pm 0.38) - 0.00026(\pm 0.00085)\ T \qquad [4]$$

valid in the temperature range of 907 to 1038 K. The corresponding equation for the straight line above the transformation temperature has been calculated by the least-square method as

$$E\ (\text{mV}) = -22.3(\pm 1.6) + 0.0255(\pm 0.0015)\ T \qquad [5]$$

in the temperature range of 1038 to 1223 K.

It has to be pointed out that in the present emf studies, no discontinuity in the emf/temperature line corsponding to the Mn(α) (pure) $\rightarrow$ Mn(β) (pure) transformation could be observed. This probably can be attributed to the small entropy change associated with this transformation, which might be within the experimental scatter.

The carbon content of the third alloy studied by the emf method was $X_C = 0.0858$. The emf values for this cell have been plotted as a function of temperature in Figure 5. The values obtained from the other cells as well as the lines corresponding to Eqs. [4] and [5] have also been drawn in the same figure for comparison. It is seen that results obtained for the cell with the alloy having a carbon content $X_C = 0.0858$ below 1038 K agree

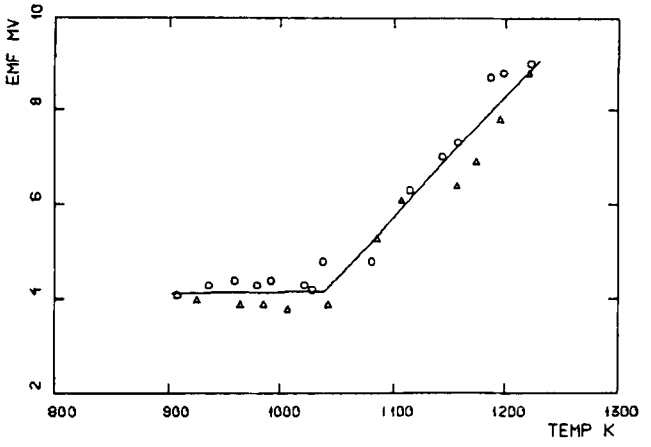

Fig. 4—The emf/temperature relationships for cells (I) and (II). ○—cell (I) and △—cell (II).

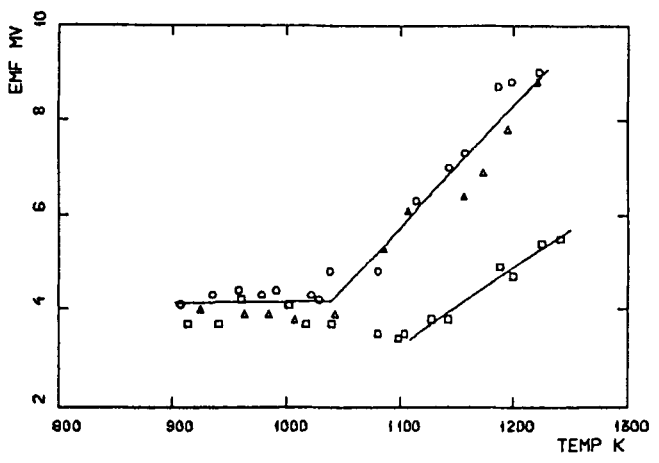

Fig. 5—The emf/temperature relationships for cells (I) through (III). ○—cell (I), △—cell (II), and □—cell (III).

well with the other two cells, thereby confirming that all three alloys lie in the same two-phase field, presumably Mn(α)-$Mn_{23}C_6$. The new equation for the straight line from all three measurements below 1038 K can be calculated by the least-square method as

$$E\ (\text{mV}) = 3.2(\pm 1.3) + 0.001(\pm 0.001)\,T \qquad [6]$$

Just above this temperature, the emf for the cell with the alloy composition $X_C = 0.0858$ shows a slight decrease up to 1110 K. Above 1110 K, the emf/temperature relationship shows a new straight line. In view of the fact that the number of experimental values between 1038 and 1110 K are very few, it was felt that a least-square equation in this region would be somewhat misleading. On the other hand, the straight line above 1110 K has been calculated to be

$$E\ (\text{mV}) = -14.88(\pm 0.26) + 0.0165(\pm 0.0002)\,T \qquad [7]$$

valid in the temperature range of 1110 to 1241 K.

A comparison of the results of the emf measurements for the alloy composition $X_C = 0.0858$ with the results of the DTA measurements in Figure 3 leads to the conclusion that this alloy would be in the Mn(α)-$Mn_{23}C_6$ two-phase field below 1038 K, in the Mn(α)-Mn(γ) two-phase field between 1038 and 1110 K, and in the Mn(γ) single-phase region above 1110 K. The cell reaction corresponding to Eq. [7] would be

$$\text{Mn}(\beta)\ (\text{pure}) = \text{Mn}(\gamma) \qquad [7a]$$

IV. DISCUSSION

The results of emf measurements seem to be in support of the phase diagram shown in Figure 3 obtained from DTA studies. However, it is not possible to confirm the three-phase reaction at 1260 K by emf technique as the highest temperature of this method was 1241 K. Beyond this temperature, the emf values were unsteady, and the results were unreliable.

The solubility of $Mn_{23}C_6$ in Mn(γ) as a function of temperature was evaluated from the results of DTA and emf measurements using a two-sublattice model.[8,10] According to this model, the standard Gibbs energy change for the formation of $Mn_{23}C_6$ from Mn(γ) and graphite is given by[10]

$$\Delta G^{\circ}_{Mn_{23}C_6} = {}^{\circ}G_{Mn_{23}C_6} - 23\,{}^{\circ}G^{\gamma}_{Mn} - 6\,{}^{\circ}G^{\text{graphite}}_{C} \qquad [8a]$$

$$\Delta G^{\circ}_{Mn_{23}C_6} = 6({}^{\circ}G_{MnC} - {}^{\circ}G^{\gamma}_{Mn} - {}^{\circ}G^{\text{graphite}}_{C} + L^{\text{Mn}(\gamma)}_{C,v}) - (12y_C - 23y_C^2)L^{\text{Mn}(\gamma)}_{C,v} + 6RT\ln y_C + 17RT\ln(1 - y_C) \qquad [8b]$$

where ${}^{\circ}G_{Mn_{23}C_6}$ = standard Gibbs energy of $Mn_{23}C_6$;
${}^{\circ}G^{\gamma}_{Mn}$ = standard Gibbs energy of Mn(γ);[10]
${}^{\circ}G^{\text{graphite}}_{C}$ = standard Gibbs energy of carbon (graphite);
${}^{\circ}G_{MnC}$ = standard Gibbs energy of the Mn-C binary (hypothetical standard state[10]);
$L^{\text{Mn}(\gamma)}_{C,v}$ = the interaction energy between carbon and vacancies in the section MnC-Mnv;[10]
$y_C = X_C/(1 - X_C)$, X_C being the mol fraction of carbon in Mn(γ) in equilibrium with the $Mn_{23}C_6$ phase at a given temperature;
R = gas constant; and
T = temperature in Kelvin.

In order to evaluate the left-hand side of Eq. [8b], the standard Gibbs energy of formation of $Mn_{23}C_6$ from pure Mn(β) and graphite was determined from earlier emf measurements,[9] *viz.*

$${}^{\circ}G_{Mn_{23}C_6} - 23\,{}^{\circ}G^{\beta}_{Mn} - 6\,{}^{\circ}G^{\text{graphite}}_{C} = -325{,}333 + 76.20\,T \ \text{J} \qquad [9]$$

${}^{\circ}G^{\beta}_{Mn}$ being the standard Gibbs energy of pure Mn(β). The standard Gibbs energy change for the reaction:

$$\text{Mn}(\beta)\ (\text{pure}) = \text{Mn}(\gamma)\ (\text{pure}) \qquad [10]$$

was estimated from the enthalpy and the temperature of transition available in literature,[11] assuming that $Cp_{\text{Mn}(\beta)} \approx Cp_{\text{Mn}(\gamma)}$. The relationship thus obtained can be represented as

$${}^{\circ}G^{\gamma}_{Mn} - {}^{\circ}G^{\beta}_{Mn} = 2120 - 1.559\,T \ \text{J}\cdot\text{mol}^{-1} \qquad [11]$$

Combining Eqs. [9] and [11] in an appropriate manner, the following relationship was obtained:

$${}^{\circ}G_{Mn_{23}C_6} - 23\,{}^{\circ}G^{\gamma}_{Mn} - 6\,{}^{\circ}G^{\text{graphite}}_{C} = -374{,}093 + 112.057\,T \ \text{J} \qquad [12]$$

An expression for the parameter $L^{\text{Mn}(\gamma)}_{C,v}$ can be derived from Eqs. [7] and [11]:

$$L^{\text{Mn}(\gamma)}_{C,v} = 83{,}501 - 91.347\,T \ \text{J}\cdot\text{mol}^{-1} \qquad [13]$$

In order to evaluate y_C values, the data from DTA measurements corresponding to the Mn(γ) − $Mn_{23}C_6$ line in Figure 3 (alloy compositions corresponding to alloys 4 through 8 and the temperatures corresponding to the second DTA peaks in Table I) were substituted along with Eqs. [12] and [13] in Eqs. [8a] and [8b]. The optimized expression thus obtained for the term (${}^{\circ}G^{\gamma}_{MnC}$ − ${}^{\circ}G^{\gamma}_{Mn}$ − ${}^{\circ}G^{\text{graphite}}_{C}$) as a function of temperature was

$${}^{\circ}G^{\gamma}_{MnC} - {}^{\circ}G^{\gamma}_{Mn} - {}^{\circ}G^{\text{graphite}}_{C} = -109{,}458(\pm 30) + 94.358(\pm 0.026)\,T \ \text{J} \qquad [14]$$

Substituting Eqs. [12], [13], and [14] in Eq. [8b], the solubility of $Mn_{23}C_6$ in Mn(γ) was calculated as a function of temperature, and this was plotted in Figure 6. The DTA results, as well as the phase-transformation points obtained from the emf measurements, have also been plotted in the same figure. The lines corresponding to the three-phase reactions, based on the DTA results, have been drawn in Figure 6 as solid lines.

An estimation of the solubility of $Mn_{23}C_6$ in Mn(γ) similar to that carried out in the present work was made earlier by Hillert and Waldenström.[10] In view of the lack of experimental data, these authors had assumed that $L_{C,v}^{Mn(\gamma)}$ had the same value as $L_{C,v}^{Fe(\gamma)}$. Nishizawa and Uhrenius[12] have also made use of the same assumption in their work. According to this assumption, the expression for $L_{C,v}^{Mn(\gamma)}$ can be represented as

$$L_{C,v}^{Mn(\gamma)} = L_{C,v}^{Fe(\gamma)} = -21{,}058 - 11.581\,T \quad J \cdot mol^{-1} \quad [15]$$

By substituting Eq. [15] in Eq. [8b], a new solubility line for the solution of $Mn_{23}C_6$ in Mn(γ) is obtained. This line is also represented in Figure 6 as a dashed line. The agreement between the two lines shows the validity of the assumption made by the earlier workers.[10,12]

The intersection between the solubility curve (line "a" in Figure 6) and the three-phase line (Mn(α), Mn(γ), $Mn_{23}C_6$) at 1031 K gives the eutectoid composition, which has been calculated as $X_C = 0.0962$. This eutectoid composition is somewhat higher than those reported in literature earlier.[1,2,5] It is to be admitted that in this estimation, a greater emphasis is laid on the DTA results than on the break points in the emf/temperature relationship in Figure 4. This was because of the fact that the present authors felt that the DTA results have a better reliability in view of the larger number of experimental points. It should be pointed out that no attempt was made in the present work to derive an expression for the solubility of Mn(α) in Mn(γ), as the number of experimental points were very few and the scatter was significant. Further experimentation may be necessary in order to evaluate this line accurately.

In order to confirm the eutectoid composition, two alloys with compositions $X_C = 0.0938$ and $X_C = 0.1012$ were melted and then furnace cooled. These alloys were examined in an optical microscope. The photomicrographs are reproduced in Figures 7 and 8. It can be seen that Figure 7 shows a small amount of Mn(α) (white areas) along with the main eutectoid structure. On the other hand, Figure 8 shows a small amount of $Mn_{23}C_6$ (large crystals in the lower-left corner) along with the dominating eutectoid structure. This would mean that the eutectoid composition would lie between these two compositions, which would agree with the estimation made in the present work, *viz.*, $X_C = 0.0962$.

The solubility curve for $Mn_{23}C_6$ in Mn(γ) calculated in the present work meets the three-phase line at 1260 K, representing the reaction:

$$\varepsilon\text{-carbide} = Mn(\gamma) + Mn_{23}C_6 \quad [16]$$

at a composition $X_C = 0.1489$, as can be seen in Figure 6. This composition is much higher than that shown in Figure 1. Nishizawa[13] has made a theoretical analysis of the ternary system Fe-Mn-C using the two-sublattice model and has presented an isothermal section (1273 K) of the ternary system. Extrapolation of the solubility line of $(Mn, Fe)_{23}C_6$ in the γ-Mn-Fe-C solution in the ternary

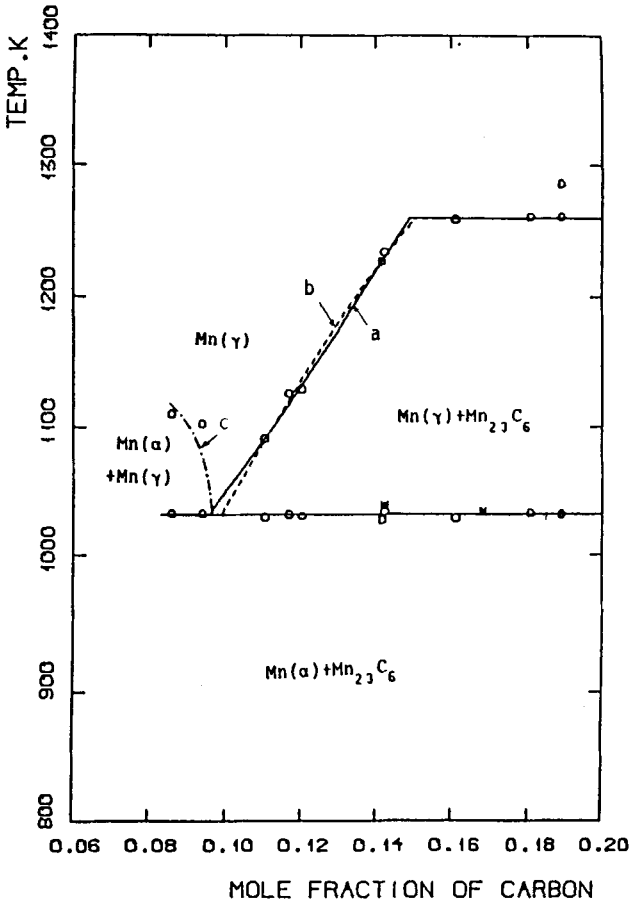

Fig. 6—The Mn-C phase diagram section proposed in the present work. Line a—calculated by using $L_{C,v}^{Mn(\gamma)}$; line b—calculated by using $L_{C,v}^{Fe(\gamma)}$; and line c—tentative line (○—DTA measurements; *—emf measurements).

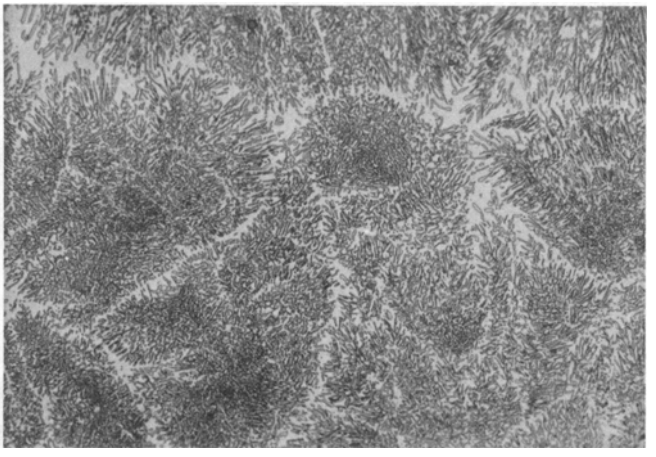

Fig. 7—Photomicrograph of an alloy with $X_C = 0.0938$ after furnace cooling (etched in 2 pct Nital). Eutectoid colonies and Mn(α) (white areas). Magnification 134 times.

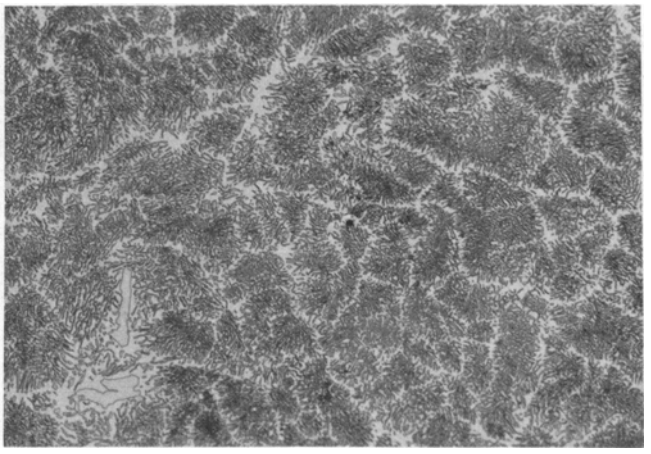

Fig. 8—Photomicrograph of an alloy with $X_C = 0.1012$ after furnace cooling (etched in 2 pct Nital). Eutectoid colonies and $Mn_{23}C_6$ (large crystals in the lower-left corner). Magnification 134 times.

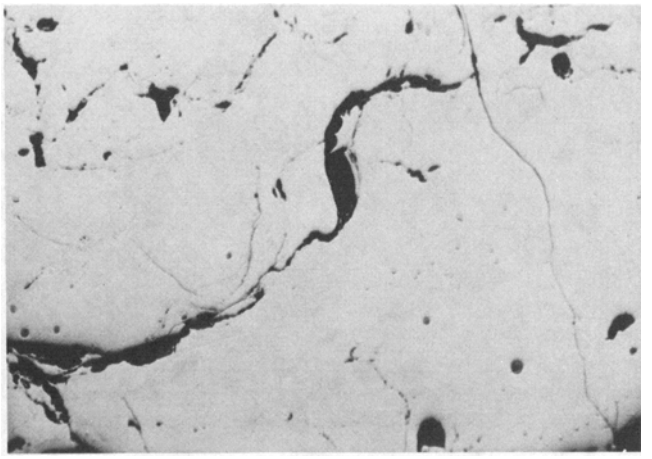

Fig. 9—Photomicrograph of an alloy with $X_C = 0.0938$ after quenching from 1189 K (etched in 2 pct Nital). Single phase: Mn(α). Magnification 119 times.

system to the Mn-C binary indicates the solubility limit at $X_C = 0.135$, which appears to be in reasonable agreement with the results of the present work.

A number of attempts were made to heat treat the Mn-C alloys at different temperatures and compositions and quench the samples so that the high-temperature phases could be identified by microscopic examination and X-ray analysis. However, no conclusive evidence could be obtained in these efforts. This is probably due to the difficulty in retaining the high-temperature phases by quenching techniques, as the phase transformations involved might be very fast. The same difficulty seems to have been faced by many earlier investigators. Isobe[2] reported that it was not possible to obtain the high-temperature structure in alloys containing 1.78 wt pct C ($X_C = 0.0766$) and 2.8 wt pct C ($X_C = 0.1165$) when the specimens were quenched in an ice-brine mixture. Kuo and Persson[3] obtained the Mn(α) phase even in samples quenched from 1323 K. Similar observations were also made by Bouchaud[6] and Lesage.[7] Benz *et al.*[4] observed Mn(α) phase in Mn-C alloy with $X_C = 0.044$ and 0.022 when quenched from temperatures above 1273 K. They further observed that an alloy containing 4.34 wt pct C ($X_C = 0.172$), when quenched from 1373 K, revealed Mn(α) and $Mn_{23}C_6$ but not Mn(γ) and $Mn_{23}C_6$ at the grain boundaries of ε-carbide.

If the Mn(γ) phase present at high temperatures gets converted to Mn(α) by means of diffusionless transformation, a sample in the Mn(γ) single-phase region at high temperatures, according to Figure 6, on quenching, is likely to result in a single Mn(α) phase. In order to verify this hypothesis, an alloy with the composition $X_C = 0.0938$ was heat treated at 1189 K and quenched. According to Figure 6, this alloy should lie in the Mn(γ) single-phase field at 1189 K. Microscopic examination of this sample showed that the specimen consisted of a single phase. The corresponding photomicrograph is given in Figure 9. X-ray analysis revealed that the phase present was Mn(α). This is in accordance with the observation of Bouchaud,[6] who obtained a single Mn(α) phase by quenching the alloy with $X_C = 0.124$ (3 wt pct) from 1273 K. At this temperature, the alloy would have consisted of a single Mn(γ) phase, according to Figure 6.

The photomicrographs of the specimens containing $X_C = 0.1727$ (4.36 wt pct) quenched from 1063 and 1189 K are given in Figures 10 and 11. Both have a similar structure, the white region being Mn(α) and the dark areas $Mn_{23}C_6$. It is likely that both the specimens were in the Mn(γ)-$Mn_{23}C_6$ two-phase region before being quenched, according to Figure 6.

In order to estimate the solubility of $Mn_{23}C_6$ in Mn(α) at temperatures below 773 K, quantitative microscopic analyses were carried out with alloys containing $X_C = 0.0938$ and $X_C = 0.1727$ after allowing them to cool slowly in the furnace itself. By assuming the difference in the molar volumes of Mn(α) and $Mn_{23}C_6$ to be negligible, the solubility can be obtained from the volume fractions of the two phases and composition of the alloy. For the alloy with $X_C = 0.0938$, the solubility was found to be 0.055 mol fraction of carbon, and for the alloy with $X_C = 0.1727$, the value was 0.059. While the agreement between the two values is good, these values are somewhat lower than that shown in Figure 1.

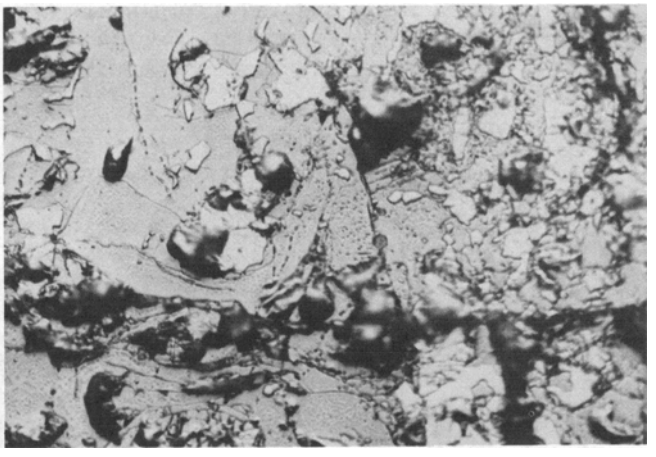

Fig. 10—Photomicrograph of an alloy with $X_C = 0.1727$ after quenching from 1063 K (etched in 2 pct Nital). White areas: Mn(α); dark areas: $Mn_{23}C_6$. Magnification 302 times.

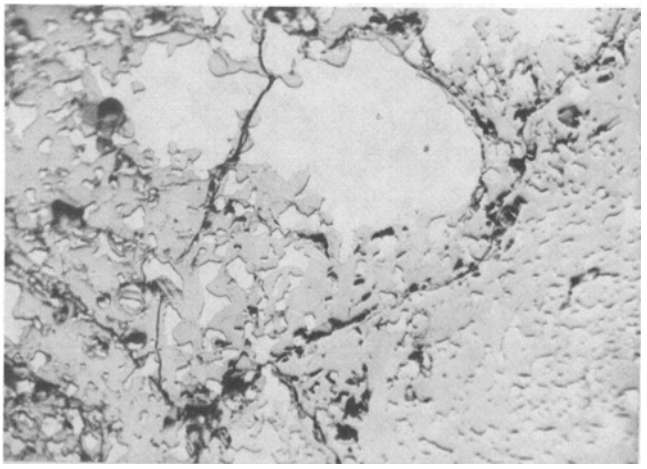

Fig. 11—Photomicrograph of an alloy with $X_C = 0.1727$ after quenching from 1189 K (etched in 2 pct Nital). White areas: Mn(α); Dark areas: $Mn_{23}C_6$. Magnification 311 times.

An equation for the activity of Mn in Mn(γ) as a function of temperature for an alloy with $X_C = 0.0858$ can be obtained by combining Eqs. [7] and [11]. This relationship can be represented as

$$\ln a_{Mn} = -0.1956 + 90.43/T \qquad [17]$$

the standard state for Mn being pure Mn(γ), as given in Eq. [8b]. Equation [17] is valid in the temperature range of 1110 to 1241 K. A similar equation for the activity of Mn in the Mn(γ)-$Mn_{23}C_6$ two-phase field can be obtained by combining Eqs. [5] and [11]. This can be represented as

$$\ln a_{Mn} = -0.4045 + 262.7/T \qquad [18]$$

the standard state being the same as for Eq. [17]. Equation [18] is valid in the temperature range of 1038 to 1223 K. The activities and activity coefficients of Mn along the Mn(γ)-$Mn_{23}C_6$ two-phase boundary line, calculated using Eq. [18], are given in Table III.

Table III. The Activities and Activity Coefficients of Mn Along the Mn(γ)-$Mn_{23}C_6$ Two-Phase Boundary Line

T, K	Mol Fraction of Mn, X_{Mn}	Activity of Mn, a_{Mn}	Activity Coefficient
1035	0.9038	0.8601	0.9517
1050	0.8999	0.8570	0.9523
1080	0.8923	0.8511	0.9538
1110	0.8850	0.8455	0.9554
1140	0.8779	0.8402	0.9571
1170	0.8710	0.8353	0.9590
1200	0.8643	0.8306	0.9610
1230	0.8577	0.8262	0.9633
1260	0.8511	0.8220	0.9658

V. SUMMARY AND CONCLUSIONS

In the present work, DTA was used to investigate some phase-diagram aspects of the Mn-C binary system around the eutectoid decomposition of Mn(γ).

The results were confirmed by emf measurements involving CaF_2 solid electrolyte. From the experimental data, the solubility of $Mn_{23}C_6$ in Mn(γ) was calculated using a two-sublattice model. A section of the Mn-C phase diagram has been put forward on the basis of the present results. The temperature for the reaction,

$$Mn(\gamma) = Mn(\alpha) + Mn_{23}C_6$$

was found to be 1031 K; the eutectoid composition was estimated to be $X_C = 0.0962$. The temperature of the three-phase reaction,

$$\varepsilon\text{-carbide} = Mn(\gamma) + Mn_{23}C_6$$

was found to be 1260 K, and the equilibrium carbon content of Mn(γ) phase was estimated to be $X_C = 0.1489$.

The results of microscopic and X-ray analyses, although inconclusive due to the difficulties in retaining the high-temperature phases on quenching, seem to be in support of the phase diagram suggested in the present work.

ACKNOWLEDGMENTS

The authors are extremely thankful to Professor Mats Hillert for his valuable suggestions during the course of this work. The authors are also thankful to Mr. Nils Lange for his help with the microscopic studies. Financial support from The Swedish Board for Technical Development (STUF) for this work is gratefully acknowledged.

REFERENCES

1. R. Vogel and W. Döring: *Arch. Eisenhüttenwes.*, 1935-36, vol. 9, pp. 247-52.
2. M. Isobe: *Sci. Rep. Res. Inst.*, Tohoku University, Sendai, Japan, 1951, Ser. A, vol. 3, pp. 468-90.
3. K. Kuo and L.E. Persson: *J. Iron Steel Inst.*, 1954, vol. 178, pp. 39-44.
4. Robert Benz, John F. Elliott, and John Chipman: *Metall. Trans.*, 1973, vol. 4, pp. 1449-52.
5. T.B. Massalski: *Binary Alloy Phase Diagrams*, 1st ed., ASM, Metals Park, OH, Oct. 1986, p. 575.
6. J.P. Bouchaud: *Ann. Chim.*, 1967, Ser. 14, vol. 2, pp. 353-66.
7. P. Lesage: *Ann. Chim.*, 1961, Ser. 13, vol. 6, pp. 623-28.
8. M. Hillert and L.-I. Staffansson: *Acta Chem. Scand.*, 1970, vol. 24, pp. 3618-26.
9. Du Sichen, S. Seetharaman, and L.-I. Staffansson: *Metall. Trans. B*, 1989, vol. 19B, pp. 951-57.
10. Mats Hillert and Mats Waldenström: *Metall. Trans. A*, 1977, vol. 8A, pp. 5-13.
11. R. Hultgren, P.D. Desai, D.T. Hawkins, M. Gleiser, K.K. Kelley, and D.D. Wagman: *Selected Values of the Thermodynamic Properties of the Elements*, ASM, Metals Park, Ohio, 1973, p. 301.
12. T. Nishizawa and B. Uhrenius: Report TRITA-MAC-0004, Dept. of Physical Metallurgy, Royal Inst. of Tech., Stockholm, Sweden, 1971.
13. T. Nishizawa: *Scand. J. Metall.*, 1977, vol. 6, pp. 74-82.